PROTEINS
STRUCTURE ■ FUNCTION ■ BIOINFORMATICS

Structure and function of a TetR family transcriptional regulator, SbtR, from *Thermus thermophilus* HB8

Yoshihiro Agari,[1] Keiko Sakamoto,[1] Katsuhide Yutani,[1] Seiki Kuramitsu,[1,2] and Akeo Shinkai[1]*

[1] RIKEN SPring-8 Center, RIKEN Harima Institute, 1-1-1 Kouto, Sayo, Hyogo 679-5148, Japan

[2] Department of Biological Sciences, Graduate School of Science, Osaka University, Toyonaka, Osaka 560-0043, Japan

ABSTRACT

SbtR is one of the four TetR family transcriptional regulators present in the extremely thermophilic bacterium, *Thermus thermophilus* HB8. We identified 10 genes controlled by four promoters with negative regulation by SbtR *in vitro*. The SbtR-regulated gene products include probable transporters, probable enzymes for sugar or amino acid metabolism, and nucleic acid-related enzymes. SbtR binds pseudopalindromic sequences, with the consensus sequence of 5′-TGACCCNNKGGTCA-3′ surrounding the promoters, and has a proposed 1:1 dimer binding stoichiometry. The X-ray crystal structure analysis revealed that SbtR comprises either nine or 10 α-helices and forms a dimer, as in the typical TetR family proteins. Similar to many characterized TetR family regulators, SbtR has a predicted ligand-binding pocket at the center of each monomer. Interestingly, the SbtR dimer contains an intermolecular disulfide bridge, formed between the Cys164 residues at the entrance of the pocket. The Cys164Ser and Cys164Ala mutant SbtR proteins formed homodimers similar to that of the wild type, but their thermal stabilities were lower by about 8°C, indicating that the disulfide bridge contributes to the thermal stability of the protein. However, altered repression activity of the mutants was not observed *in vitro*. From these results, we propose that ligand-binding is essential for SbtR to disengage from DNA, in a similar manner to the other characterized TetR family regulators. The formation and reduction of the disulfide bond might function in controlling the ligand-binding affinity of this transcriptional regulator.

Proteins 2013; 81:1166–1178.

Key words: BIAcore; disulfide bridge; DSC; functional genomics; genomic SELEX; ITC; structural genomics; thermal stability; thermophile; transcription factor.

INTRODUCTION

TetR family transcriptional regulators are one of the major families of bacterial transcriptional regulators.[1–3] Most of the TetR family regulators are repressors that control various genes, such as those involved in multidrug resistance, catabolic pathways, antibiotic biosynthesis, osmotic stress, and pathogenicity.[2] They bind their operators, composed of ~10–30-bp palindromic sequences, to repress the target genes, and derepression occurs when the regulators bind their cognate ligands.[4] While the amino acid sequences of the N-terminal helix-turn-helix (HTH) DNA-binding domains share high similarity among the family members, those of the C-terminal ligand-binding domains are diverse.[2,4] However, all of the characterized TetR family proteins form dimers with a similar domain structure, composed of ~10 α-helices per monomer.[4] Two mechanisms of derepression by the TetR family repressors have been proposed. One involves the ligands binding around the center of the repressor molecules, causing the proteins to undergo a conformational change that increases the distance between the DNA recognition helices, and thereby dissociating the protein from the DNA.[5–7] The other involves the ligand-binding capture of one of the apo-repressors in a conformation that is not compatible with DNA binding, rather than the induction of a conformational change.[8,9] A TetR family protein from *Streptomyces coelicolor* A3(2), γ-butyrolactone autoregulator receptor protein CprB,

Additional Supporting Information may be found in the online version of this article.

Grant sponsor: Ministry of Education, Culture, Sports, Science and Technology, Japan; Grant number: 22510208.

*Correspondence to: Akeo Shinkai, RIKEN SPring-8 Center, RIKEN Harima Institute, 1-1-1 Kouto, Sayo, Hyogo 679-5148, Japan. E-mail: ashinkai@spring8.or.jp

Received 3 October 2012; Revised 19 January 2013; Accepted 29 January 2013
Published online 14 February 2013 in Wiley Online Library (wileyonlinelibrary.com). DOI: 10.1002/prot.24266

which controls actinorhodin and undecylprodigiosin biosynthesis and/or morphogenesis, forms an intermolecular disulfide bridge at the interface of the dimer molecules; however, the role of the disulfide bridge in the protein's function has not been elucidated.[10]

The thermophilic bacterium *Thermus thermophilus* HB8[11] is considered to represent a minimal model of life, because of its relatively small genome (NCBI accession numbers NC_006461, NC_006462, and NC_006463).[12] Therefore, various structural and functional genomics studies have been performed with this strain (http://www.thermus.org/e_index.htm). Based on the genome sequence analysis, this strain is predicted to encode ~70 transcriptional regulators, but only a few of them have been characterized. *T. thermophilus* HB8 encodes four TetR family proteins, TTHA0101 (FadR),[13] TTHA0167, TTHA0973 (PaaR),[14] and TTHB023 (PfmR)[15] (NCBI accession numbers YP_143367.1, YP_143433.1, YP_144239.1, and YP_145262.1, respectively), which share 44–57% amino acid sequence similarity with each other. In this study, we characterized the structure and function of the TTHA0167 protein. The structural analysis revealed that the recombinant TTHA0167 protein has an intermolecular disulfide bridge at the dimer interface, and thus we investigated the role of this disulfide bridge.

MATERIALS AND METHODS

Expression plasmid construction

The *TTHA0167* (*sbtR*) gene was amplified by genomic PCR, using the primers P01 and P02 (Supporting Information Table SI). The amplified fragment was cloned under the control of the T7 promoter (*Nde*I-*Bam*HI sites) in the *E. coli* expression vector pET-11a (Merck), to construct pET-sbtR (RIKEN BioResource Center: http://www.brc.riken.jp/inf/en/index.shtml). The first and second codons, GTG and GCC, of the open reading frame (ORF) found in the chromosome were converted to ATG and GCT, respectively, in the expression plasmid. To construct the expression plasmid pET-sbtR_his, encoding SbtR fused with a $(His)_6$ tag at its C terminus, PCR was performed using pET-sbtR as the template, with P03 and P04 as primers (Supporting Information Table SI), and the amplified fragment was cloned under the control of the T7 promoter (*Nde*I-*Bam*HI sites) in the *E. coli* expression vector pET-21a(+).

Purification of recombinant SbtR proteins

E. coli BL21(DE3) cells (Merck) harboring pET-sbtR were cultured at 37°C in 6 L of Luria-Bertani (LB) broth, containing 50 μg ampicillin mL^{-1}, for 16 h. The cells (17 g) were resuspended in 60 mL of 20 m*M* Tris-HCl (pH 8.0), containing 50 m*M* NaCl, and were disrupted by sonication in ice water. The same volume of buffer, preheated at 70°C, was added to the cell lysate. This mixture was incubated for 10 min at 70°C, and then ultracentrifuged (200,000*g*) for 1 h at 4°C. The supernatant was applied to a RESOURCE PHE column (GE Healthcare), pre-equilibrated with 50 m*M* sodium phosphate buffer (pH 7.0) containing 1.5 *M* $(NH_4)_2SO_4$, and then the bound protein was eluted with a linear gradient of 1.5–0 *M* $(NH_4)_2SO_4$. The target fractions were collected, and the buffer was exchanged by fractionation on a HiPrep 26/10 desalting column (GE Healthcare), pre-equilibrated with 20 m*M* MES (pH 6.0) containing 50 m*M* NaCl. The sample was then applied to a RESOURCE S column (GE Healthcare), pre-equilibrated with the same buffer, and the bound protein was eluted with a linear gradient of 0.05–0.5 *M* NaCl. The target fractions were collected and desalted by fractionation on a HiPrep 26/10 desalting column, pre-equilibrated with 10 m*M* sodium phosphate buffer (pH 7.0) containing 150 m*M* NaCl. The sample was then applied to a hydroxyapatite CHT10-I column (BIO-RAD), pre-equilibrated with the same buffer, and the bound protein was eluted with a linear gradient of 0.01–0.25 *M* sodium phosphate. The target fractions were collected, and applied to a HiLoad 16/60 Superdex 200 pg column (GE Healthcare), pre-equilibrated with 20 m*M* Tris-HCl (pH 8.0) containing 0.15 *M* NaCl. The target fractions were collected, and concentrated with a Vivaspin 20 concentrator (5,000 molecular weight cut-off, Sartorius). The Cys164Ser (C164S) and Cys164Ala (C164A) mutant SbtR proteins were purified in basically the same manner as the wild-type protein (see above). The selenomethionine-containing recombinant SbtR (Se-SbtR) protein was generated, using the *E. coli* methionine auxotroph B834(DE3) (Merck) as the host. The recombinant strain was grown in LeMaster medium,[16] containing 50 μg SeMet mL^{-1} and 50 μg ampicillin mL^{-1}, for 16 h. Se-SbtR was purified in basically the same manner as the native protein (see above).

SbtR with the C-terminal $(His)_6$ tag (SbtR-His) was expressed in *E. coli* BL21 (DE3) (Merck) harboring pET-sbtR_his. The cells were cultured at 37°C in 0.2 L of LB broth, containing 50 μg ampicillin mL^{-1}, for 16 h. The cells (0.6 g) were resuspended in 24 mL of 20 m*M* Hepes-NaOH (pH 7.5) containing 0.5 *M* NaCl, and were disrupted by sonication in ice water. The cell lysate was incubated for 10 min at 70°C, and then centrifuged (18,400*g*) for 30 min at 4°C. The supernatant was applied to a HisTrap HP column (GE Healthcare), pre-equilibrated with 20 m*M* Hepes-NaOH (pH 7.5) containing 0.5 *M* NaCl and 5 m*M* imidazole, and then the bound protein was eluted with a linear gradient of 5–500 m*M* imidazole. The target fractions were collected, and applied to a HiLoad 16/60 Superdex 200 pg column, pre-equilibrated with 20 m*M* Tris-HCl (pH 8.0) containing 0.15 *M* NaCl. The target fractions were collected, and concentrated with a Vivaspin 20 concentrator (5,000 molecular weight cut-off, Sartorius). The protein

Table I
X-Ray Data Collection and Refinement Statistics

	SeMet	Native
Data collection		
Source	BL26B2 (SPring-8)	BL26B2 (SPring-8)
Wavelength (Å)	0.9793	1.0
Resolution (Å)	50–2.70 (2.78–2.70)	50–2.04 (2.09–2.04)
Space group	$P2_1$	$P2_1$
No. of molecules in an asymmetric unit	4	4
Unit cell parameters (Å, °)	$a = 44.66$, $b = 178.70$, $c = 56.44$ $\alpha = 90$, $\beta = 92.37$, $\gamma = 90$	$a = 44.33$, $b = 174.82$, $c = 56.16$ $\alpha = 90$, $\beta = 92.43$, $\gamma = 90$
No. of measured reflections	179,177	225,048
No. of unique reflections	23,697	53,147
Completeness (%)	97.5 (100)	98.2 (79.1)
Redundancy	7.6 (7.3)	4.2 (4.1)
I/σ (I)	19.1 (6.4)	29.1 (5.8)
R_{merge}[a] (%)	8.9 (31.5)	4.6 (26.6)
Refinement		
Resolution range (Å)		30.3–2.05
R_{work}[b] (%)/R_{free}[c] (%)		20.1/25.0
No. of unique reflections used in the R_{free} set		46919
No. of protein atoms / water atoms		5,767/296
Wilson B factor (Å^2)		22.8
Average B factors (Å^2) for protein/water		35.0/38.5
r.m.s.d. bond lengths (Å)		0.009
r.m.s.d. bond angles (°)		1.2
Ramachandran analysis[d]		
Favored (%)		98.1
Outliers (%)		0.0

Values in parentheses are for the highest-resolution shell.[a]$R_{merge} = \Sigma_h\Sigma_i|I_{h,i}-<I_h>|/\Sigma_h\Sigma_i I_{h,i}$, where $I_{h,i}$ is the ith measured diffraction intensity of reflection h and $<I_h>$ is the mean intensity of reflection h.[b]R_{work} is the R-factor $= \Sigma||F_o|-|F_c||/\Sigma|F_o|$, where F_o and F_c are the observed and calculated structure factors, respectively.[c]R_{free} is the R-factor calculated using 10% of the data that were excluded from the refinement.[d]Calculated by MolProbity.

concentrations were determined by measuring the absorbance at 280 nm.[17]

The Se-SbtR protein was crystallized and used for the phasing of X-ray diffraction data. The SbtR-His protein was used for the Genomic SELEX, and the native SbtR protein was used for all other experiments.

Crystallization and X-ray crystal structure analysis of SbtR

The crystal used for the single-wavelength anomalous dispersion (SAD) phasing was obtained by the oil-batch method at 293 K, by mixing 2.0 μL of recombinant Se-SbtR (15.8 mg mL^{-1}), obtained as described above, with 1.0 μL of a crystallization solution, containing 0.2 *M* phosphate-citrate (pH 4.2) and 30% (v/v) PEG 300. The mixture was then covered with 15 μL of silicone and paraffin oil. Crystals grew within 4 days to maximum dimensions of 100 × 50 × 20 μm^3. The crystal was mounted on a cryoloop, and flash-cooled in a nitrogen gas stream at 100 K. The diffraction dataset was obtained at 0.9793 Å with an MX-225 charge-coupled device (CCD) detector (Rayonix LLC), using the Structural Genomics Beamline II synchrotron (BL26B2)[18] at SPring-8 (Hyogo, Japan) (proposal number 20120012). The oscillation angle was 1.0°, the exposure time was 4 s per frame, and the camera distance was 230 mm. The crystal used for the refinement was obtained by the oil-batch method at 293 K, by mixing 2.0 μL of recombinant nonlabeled SbtR (7.1 mg mL^{-1}) with an equal volume of crystallization solution, containing 0.2 *M* phosphate-citrate (pH 4.6), 30% (v/v) PEG 300 and 0.15 *M* lithium chloride. The mixture was then covered with 15 μL of silicone and paraffin oil. The native dataset was obtained by basically the same procedure as that used for Se-SbtR, except that the wavelength was 1.0 Å, the exposure time was 15 s per frame, and the camera distance was 210 mm. The data were processed with the HKL2000 program suite.[19] The selenium sites were determined with the SOLVE program,[20] and the resulting phases were improved with the RESOLVE program.[20] The initial model was built with the ARP/wARP program[21] in the CCP4 suite,[22] and further manual model building was performed with Coot.[23] Simulated annealing, energy minimization, and B factor refinement were performed using the CNS program package.[24] Cycles of manual modeling and CNS refinement were performed, and 10% of the total reflections were randomly chosen for the R_{free} sets. The quality of the structure was validated using the ADIT! Validation Server in PDBj (http://pdbdep.protein.osaka-u.ac.jp/validate/en/) and the MolProbity server (http://molprobity.biochem.duke.edu/). The data collection and refinement statistics are presented in Table I.

Genomic SELEX

The genomic SELEX search for the SbtR-binding sequence was performed in basically the same manner as described previously.[14,25] The *T. thermophilus* HB8 genomic DNA library plasmids comprised 5×10^4 independent clones, carrying ~0.1–0.3-kbp DNA fragments.[14] PCR was performed using the DNA library plasmids,[14] and the amplified fragments were excised from a 1% agarose gel. Approximately 10 pmol (1.3 μg) of the DNA fragment and 20 pmol of the SbtR-His dimer were mixed in 0.1 mL of buffer A, comprising 20 m*M* Tris-HCl (pH 7.7), 3 m*M* magnesium acetate, 0.2 *M* KCl, and 1.25 μg bovine serum albumin mL^{-1}, and incubated for 20 min at 55°C. The nickel resin (0.1 mL: ProBond Resin, Invitrogen), pre-equilibrated with buffer A, was added to the sample, and the mixture was incubated for 20 min at 55°C. The mixture was transferred to a column, which was washed with 5 mL of buffer A containing 5 m*M* imidazole, and the bound sample was eluted with 0.25 mL of buffer A containing 250 m*M* imidazole. The DNA was extracted from the eluted sample with phenol and ether. PCR was performed with the extracted DNA, as described previously.[14] The amplified fragments were purified by using a QIAquick PCR purification kit (QIAGEN), and were used for the next round of genomic SELEX. The selected DNA fragments were cloned into the pGEM-T-easy plasmid (Promega), and the nucleotide sequences were analyzed.

ITC measurements

Isothermal titration calorimetry (ITC) measurements were performed at 15°C, using a MicroCal Auto-iTC$_{200}$ (GE Healthcare). The SbtR monomer (100 μ*M*), in 20 m*M* Tris-HCl (pH 8.0) containing 0.15 *M* NaCl, was placed in the syringe and titrated into 0.2 mL of 5 μ*M* double-stranded (ds)DNA in the same buffer. Aliquots (2 μL) of the SbtR solution were injected 18 times at 0.067 μL s^{-1}, with a 4.2 min interval between the injections. The baseline was corrected by subtracting the trace of buffer injections from the raw calorimetric trace. The nonlinear one-site model was fit to the base-line-corrected raw ITC data, to determine the binding constant (K_b) value and the ligand binding stoichiometry, using the ORIGIN (ver. 7.0) software (GE Healthcare).

BIAcore biosensor assay

A dsDNA fragment (0.1 m*M*), biotinylated at the 5′ end of one strand, was diluted to 50 n*M* in 10 m*M* Hepes-NaOH (pH 7.4) buffer, containing 0.5 *M* NaCl, 3 m*M* EDTA, and 0.005% surfactant P20, and then applied to an SA biosensor chip (GE Healthcare), as described previously.[14] All experiments for measuring the DNA and SbtR interactions were performed at 15 or 25°C, using buffer A [10 m*M* Hepes-NaOH (pH 7.4), 0.3 *M* NaCl, 3 m*M* EDTA, 0.005% surfactant P20]. The protein was diluted with the same buffer, and then injected over the DNA surface at a flow rate of 20 μL min^{-1}. Sensorgrams were recorded and normalized to a baseline of 0 response units (RU). An equivalent volume of each protein dilution was also injected over a nontreated surface, to determine the bulk refractive index background. At the end of each cycle, the bound protein was removed by injecting 80 μL of 3 *M* NaCl, to regenerate the chip. The association and dissociation rate constants (k_{on} and k_{off}, respectively), and the dissociation constant (K_d) values were determined by 1:1 Langmuir local fitting with the BIAevaluation 3.0 software (GE Healthcare).

In vitro transcription assay

Preparation of templates

The construction of the plasmids containing the upstream regions of the *TTHA0027* and *TTHA0787* genes was performed in basically the same manner as described previously,[26] using the oligonucleotides P05/P06 and P07/P08, respectively (Supporting Information Table SI). The upstream regions of the *TTHA1821* and *TTHA1822* genes were amplified by genomic PCR, using the primers P09/P10 and P11/P12, respectively (Table SI). The amplified fragments were digested with *Bam*HI and *Eco*RI, and were cloned into pUC19 (Novagen). Using each plasmid as the template, PCR was performed with the primers P13 and P14 (Table SI) to prepare the template DNA for the transcription assay.

Run-off transcription

Assays were performed in 15-μL reaction mixtures, in the absence or presence of the transcription factor, in basically the same manner as described previously.[26] The template DNA was preincubated with or without SbtR at 55°C for 5 min. *T. thermophilus* RNA polymerase-σ^A holoenzyme (RNAP), purified as reported previously,[27] was added, and the mixture was further incubated for 5 min. Transcription was initiated by the addition of 1.5 μCi [α-^{32}P]CTP and unlabeled ribonucleotide triphosphates. After an incubation for 10 min, the reactions were stopped. The samples were fractionated on a 10% polyacrylamide gel containing 8 *M* urea, and analyzed by autoradiography.

Identification of the transcriptional start site

Total RNA, isolated from wild-type *T. thermophilus* HB8 cells cultured at 70°C in rich medium, was treated with DNase I, followed by ethanol precipitation.[26] Rapid amplification of cDNA ends (5′-RACE) was performed with a 5′-Full RACE Core Set (Takara Bio), as described previously.[14] The first strand cDNA was synthesized with the 5′-phosphorylated primers P15, P16, P17, and P18 for the *TTHA0027*, *TTHA0787*, *TTHA1821*, and *TTHA1822*

genes, respectively (Supporting Information Table SI). The RNA was digested by RNaseH, and the single-stranded cDNA was ligated with T4 RNA ligase to construct DNA concatemers. PCR was performed using the DNA concatemers as templates, and P19/P20, P21/P22, P23/P24, and P25/P26 (Table SI) as primers for the *TTHA0027*, *TTHA0787*, *TTHA1821*, and *TTHA1822* genes, respectively. The second PCR was performed using the primers P27/P28, P29/P30, P31/P32, and P33/P34 (Table SI) for the *TTHA0027*, *TTHA0787*, *TTHA1821*, and *TTHA1822* genes, respectively. The amplified DNA fragments were cloned into the plasmid pT7Blue (Merck), and the nucleotide sequences of several clones for each gene were analyzed.

RT-PCR

Total RNA, isolated from the wild-type *T. thermophilus* HB8 strain cultured in rich medium, was treated with DNase I, followed by ethanol precipitation.[26] Using the RNA (1–5 μg) as the template, reverse transcription (RT) was performed using a PrimeScript RT-PCR kit (Takara Bio).[14] Subsequently, using the reaction mixture (1 μL) as the template, PCR was performed in the presence of 0.2 μ*M* of each primer (Supporting Information Table SI), in a 25 μL reaction mixture. Primers P35 and P36, which correspond to the genome positions 754,389–754,372 and 752,735–752,718, respectively, were used to detect the operon including the *TTHA0787–TTHA0785* genes. The PCR analysis involved 40 cycles, at 94°C for 30 s, 57°C for 30 s, and 72°C for 2 min, in GC buffer II (Takara Bio). Primers P37 and P38, which correspond to the genome positions 1,704,541–1,704,517 and 1,702,131–1,702,107, respectively, were used to detect the operon composed of the *TTHA1821–TTHA1818* genes. The PCR analysis involved 30 cycles, at 96°C for 40 s, 60°C for 30 s, and 72°C for 4 min, in GC buffer II. Primers P39 and P40, which correspond to the genome positions 1,705,283–1,705,300 and 1,706,790–1,706,807, respectively, were used to detect the operon composed of the *TTHA1822–TTHA1823* genes. The PCR analysis involved 40 cycles, at 94°C for 30 s, 57°C for 30 s, and 72°C for 2 min, in GC buffer II. To confirm the absence of genomic DNA contamination of the total RNA fraction used as the template, PCR was performed with no RT, as a control.

Site-directed mutagenesis

Site-directed mutagenesis was performed on the plasmid pET-sbtR, using a QuikChange site-directed mutagenesis kit (Stratagene) with the primers P41/P42 or P43/P44 (Supporting Information Table SI).

DSC measurements

Differential scanning calorimetry (DSC) was performed using a Microcal-VP-capillary DSC platform (GE Healthcare). The protein samples were dialyzed for at least 14 h against 20 m*M* potassium phosphate (pH 7.0), containing 0.15 *M* NaCl and 1 m*M* EDTA. The samples were filtered through 0.22-μm pore membranes following dialysis, and were degassed before measurements. The protein concentrations were typically around 1.0 mg mL^{-1}. The heating rate (scan rate) of the DSC measurements was 1°C min^{-1}.

Other methods

The N-terminal sequence of the protein was analyzed with a protein sequencer (Procise HT; Applied Biosystems). To estimate the molecular mass of SbtR, the protein was subjected to gel filtration chromatography on a Superdex 75 HR 10/30 column (GE Healthcare). The BLAST search was performed on the website http://blast.ncbi.nlm.nih.gov/Blast.cgi. The nucleotide sequence motif search was performed with the GENETYX program, ver. 8.0 (GENETYX).

Data deposition

The atomic coordinates and structure factors have been deposited in the Protein Data Bank (PDB), under the accession number 3VUQ.

RESULTS

Initial characterization of the TTHA0167 protein (SbtR)

The TTHA0167 protein consists of 189 amino acid residues (NCBI accession number YP_143433.1), with a predicted molecular mass of 21.5 kDa. The BLAST search revealed that the protein has a conserved domain of the TetR family transcriptional regulators, comprising residues Ile19–Leu65 (Ile17–Leu63 in Fig. 1), with an *E* value of 2.72e-14 for the consensus sequence (pfam00440). The TTHA0167 protein contains a cysteine residue (Cys164) in the C-terminal domain (Fig. 1). According to the BLAST search, several homologs from *Thermus* species, with *E* values of 4e-129 to 8e-100 and sequence identities (IDE) of 100–90%, have corresponding cysteine residues. We found that several homologs from other species, such as *Meiothermus*, *Marinithermus*, *Oceanithermus*, *Clostridium*, *Limnobacter*, *Alcaligenes*, *Syntrophobacter*, and *Azoarcus*, with *E* values of 2e-31 to 1e-22 and IDE of 56–22%, also contain the cysteine residues (Fig. 1). The TTHA0167 protein shares homology with the *T. thermophilus* TetR family regulators FadR, PaaR, and PfmR, which lack cysteine residues, with *E* values of 7e-06, 6e-07, and 8e-04 (IDE of 33, 26, and 25%), respectively.

The TTHA0167 protein was overexpressed in *E. coli*, and the recombinant protein was purified from the cell lysate. The lysate was subjected to heat treatment at 70°C for 10 min, and after centrifugation, the supernatant was fractionated on a hydrophobic column. This step was followed by cation exchange, hydroxyapatite, and gel-filtration

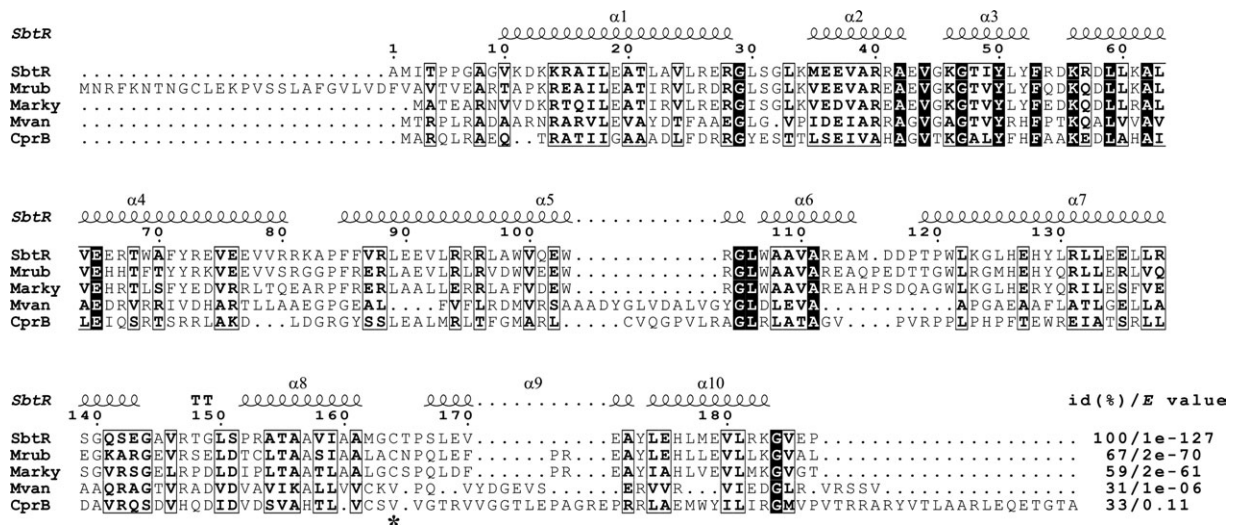

Figure 1

Sequence alignment of *T. thermophilus* SbtR with representative homologous proteins. Strictly conserved residues are represented by white letters on a black background, and similar residues are depicted by boxed bold letters. Mrub, *Meiothermus ruber* DSM 1279 Mrub_0464 (YP_003506261.1); Marky, *Marinithermus hydrothermalis* DSM 14884 Marky_2031 (YP_004368869.1); Mvan; *Mycobacterium vanbaalenii* PYR-1 Mvan_0763 (YP_951607.1), CprB; *Streptomyces coelicolor* A3 CprB (NP_630180.1). The sequences were aligned using Clustal Omega.[28,29] The secondary structure of SbtR (chain C) was calculated with DSSP,[30] and the figure was generated with ESPript 2.2.[31] α and T represent α-helix and turn, respectively. The percentage identities [id.(%)] and the *E* values relative to SbtR, determined by the BLAST analysis, are indicated on the right. The position of Cys164 in SbtR is denoted by an asterisk.

column chromatography steps. The N-terminal amino acid sequence of the purified protein was Ala-Met-Ile-Thr-Pro, indicating that the purified protein is TTHA0167 and its N-terminal two amino acid residues were removed (data not shown). The molecular mass of the TTHA0167 protein, as estimated by gel-filtration chromatography, was ~40 kDa, suggesting that the TTHA0167 protein exists as a homodimer in solution (Supporting Information Fig. S1). A sodium dodecyl sulfate (SDS)-polyacrylamide gel electrophoresis (PAGE) analysis under nonreducing conditions revealed two bands: a ~40 kDa main band and a ~25 kDa band, with a molar ratio of about 4 : 1 (Fig. 2, lane 2). The relative amount of the lower band increased with higher concentrations of dithiothreitol (DTT), suggesting that the upper band corresponds to the TTHA0167 homodimer formed by disulfide bonding, while the lower band corresponds to the monomers arising from dimer dissociation under reducing conditions. The TTHA0167 homodimer was not completely converted to the monomer even in the presence of an excess amount of DTT (Fig. 2, lane 5). Because the TTHA0167 protein has an intermolecular disulfide bridge, we named this protein *T. thermophilus* SbtR (inter-molecular disulfide-bridge-containing TetR family regulator).

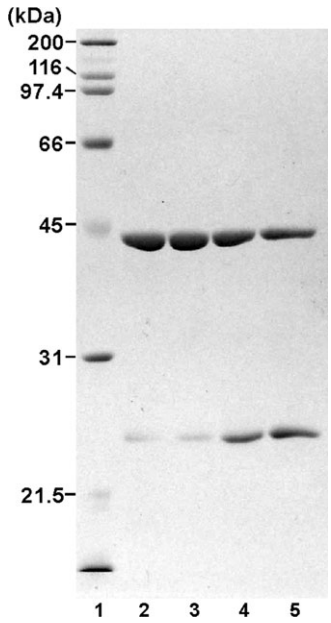

Figure 2

SDS-PAGE analysis of SbtR. Samples (1.5 μg each) of recombinant SbtR, in the absence (lane 2) or presence of 1 m*M* (lane 3), 10 m*M* (lane 4), or 100 m*M* (lane 5) DTT, were fractionated on a 12% polyacrylamide gel, which was stained with Coomassie Brilliant Blue R-250. Lane 1, molecular mass markers.

Screening of SbtR-binding sequences

To identify the genes regulated by SbtR, genomic SELEX was performed to screen for DNA fragments that bind SbtR. In this experiment, we used the SbtR_His protein,

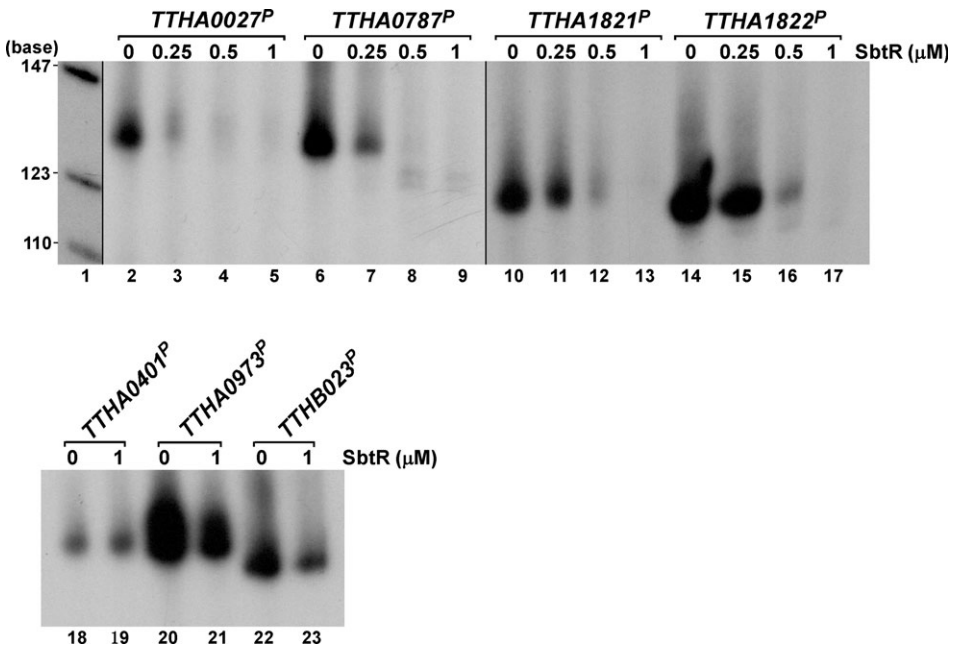

Figure 3

Effects of *T. thermophilus* SbtR on transcription *in vitro*. Run-off transcription assays were performed with templates containing the promoter regions of the genes regulated by SbtR (*TTHA0027*^{P}, *TTHA0787*^{P}, *TTHA1821*^{P}, and *TTHA1822*^{P}), FadR (*TTHA0401*^{P}),[13] PaaR (*TTHA0973*^{P}),[14] and PfmR (*TTHB023*^{P}),[15] in the absence or presence of SbtR. After the reactions, the samples were fractionated by polyacrylamide gel electrophoresis, followed by autoradiography. Lane 1, [α-^{32}P]dCTP-labeled *Msp*I fragments of pBR322.

linked to a nickel resin column, to select the DNA fragments. We confirmed that the SbtR_His protein exhibited similar transcriptional repression activity to that of the native SbtR *in vitro* (data not shown). The DNA fragments that bound to SbtR_His were selected from the *T. thermophilus* HB8 genomic library. We cloned the DNA fragments selected after four rounds of genomic SELEX, because the DNA fragments isolated after more than five rounds ran as smeared patterns on the agarose gel and were difficult to clone. Among the selected clones, the nucleotide sequences of 46 clones were analyzed (Supporting Information Table SII), and 13 clones contained genomic sequences from *T. thermophilus* HB8. Most of the others may be artifacts generated during the genomic SELEX process. Out of the 13 clones, 10 contained upstream portions of genes, and three were from ORFs. The upstream portions were those from the *TTHA1316* (six clones), *TTHA0787* (two clones), *TTHA0027* (one clone), and *TTHA0760* (one clone) genes, and included similar palindromic or pseudopalindromic sequences; that is, the potential transcription factor binding sites 5′-TGACCGGTCA-3′, 5′-TGACCCGCGGGTCA-3′, 5′-TGACCCGCTGGTCA-3′, and 5′-TGACCCAAATGCCC-3′, respectively (Supporting Information Table SII).

Identification of SbtR target genes

To confirm the SbtR target genes, we investigated the effects of SbtR on transcription *in vitro*. DNA fragments containing the aforementioned potential transcription factor binding sites were constructed, and used as templates. We found that the templates containing the upstream portions of the *TTHA0027* and *TTHA0787* genes were transcribed by *T. thermophilus* RNAP, and that SbtR repressed the transcription reactions (Fig. 3, lanes 2–9). The template containing the upstream portions of the *TTHA1316* gene was transcribed by RNAP, but transcriptional repression by the SbtR was not observed (data not shown). The transcripts from the template containing the upstream portions of the *TTHA0760* gene were not detected (data not shown). These results suggested that *TTHA0027* and *TTHA0787* are regulated by SbtR. The SbtR protein did not significantly affect the transcription of the genes regulated by the other TetR family regulators, including FadR, PaaR, and PfmR, *in vitro* (Fig. 3, lanes 18–23).

Next, we performed ITC measurements to investigate the ability of SbtR to bind dsDNAs with the aforementioned pseudopalindromic sequence. A typical thermogram was obtained when SbtR was titrated into the solution of the DNA fragment, containing the upstream regions of the *TTHA0027* gene (5′-AGCGACTGACCCGCTGGTCAATC CCG-3′) (predicted SbtR-binding sequence is underlined) [Fig. 4(A), upper panel]. The K_b value (1.6×10^7 M^{-1}) (K_d value: 63 nM) and the number of binding sites on DNA (∼1.8 sites for SbtR monomer) were obtained from the nonlinear one-site model to the normalized fitting

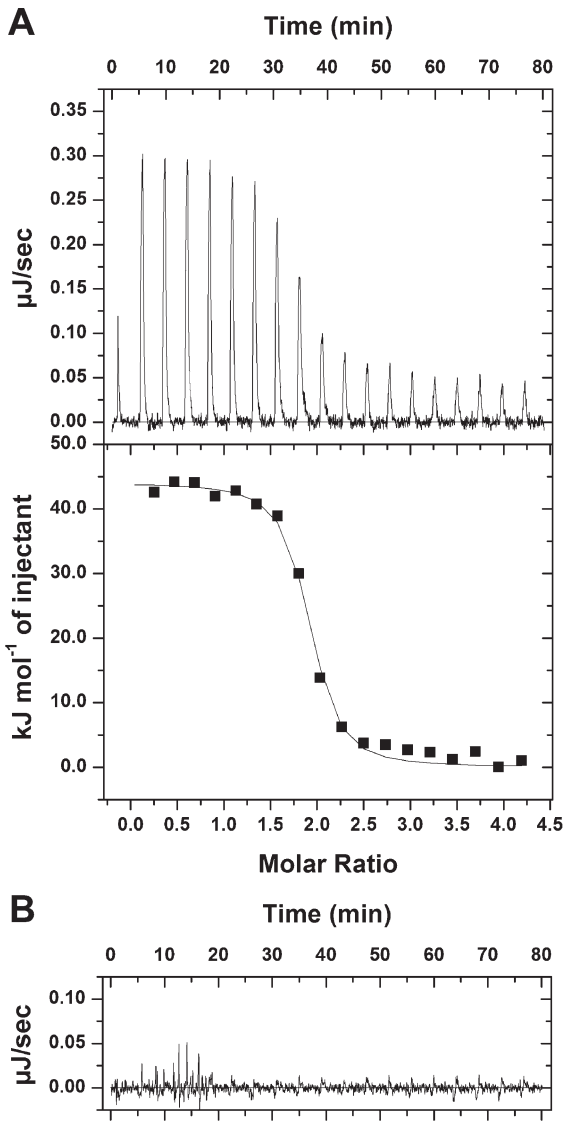

Figure 4

ITC profiles of titrations of *T. thermophilus* SbtR with the dsDNA fragment corresponding to the upstream region of the *TTHA0027* gene containing the predicted SbtR-binding site (**A**), and the fragment of the *TTHA0890* gene[13] containing the predicted FadR-binding site (**B**). The raw thermograms are shown. The lower panel in panel A indicates the titration curve fitted to the one-site mode.

curve [Fig. 4(A), lower panel]. A thermogram indicating no molecular interaction was obtained when the DNA fragment containing the binding site of *T. thermophilus* FadR[13] was used [Fig. 4(B)]. Specific DNA binding by SbtR was also observed by means of a BIAcore analysis (Supporting Information Fig. S2), although the K_d value determined from this analysis was lower than that from the ITC measurement; i.e., 11 n*M* at 15°C or 5.8 n*M* at 25°C. Together, these results indicated that SbtR specifically binds to the pseudopalindromic sequence found upstream of the *TTHA0027* and *TTHA0787* genes, with a proposed 1:1 dimer binding stoichiometry, to repress the target genes.

To find other possible SbtR-binding sites, we searched for potential binding sites in the whole genome of *T. thermophilus* HB8, by using the consensus sequence (5′-TGACCNNNNGGTCA-3′) as a query. The results revealed six sequences besides the upstream portions of the *TTHA0027* and *TTHA0787* genes. Two of them were the upstream portions of the *TTHA1330* (5′-TGACCCGT TGGTCA-3′) and *TTHA1822* (5′-TGACCAAAGGGTCA-3′) genes, and the others were from the ORFs of the *TTHA0579* (5′-TGACCCGCCGGTCA-3′), *TTHA1325* (5′-TGACCTCTTGGTCA-3′), *TTHA1342* (5′-TGACCGACC GGTCA-3′), and *TTHA1851* (5′-TGACCGGCGGGTCA-3′) genes. We confirmed that the transcription of the DNA fragment containing the upstream region of the *TTHA1822* gene, including the predicted SbtR-binding site, was repressed by SbtR (Fig. 3). We also observed similar transcriptional repression of a DNA fragment containing the upstream portion of the *TTHA1821* gene, which resides upstream of the *TTHA1822* gene in the opposite direction (Fig. 3), suggesting that SbtR binds between the *TTHA1821* and *TTHA1822* genes and represses the transcription of both genes. SbtR did not regulate the transcription of a DNA fragment containing the upstream portion of the *TTHA1330* gene *in vitro* (data not shown). The predicted SbtR-binding site upstream of the *TTHA1330* gene may not overlap with its promoter. The *in vitro* analysis revealed that SbtR did not regulate the transcription of the DNA fragments containing the upstream region of its own (*TTHA0167*) gene, the *TTHA0164* gene, and the *TTHA0166-0165* operon, which are located close to the *sbtR* gene (NCBI accession numbers NC_006461) (data not shown). In total, we identified four promoters that are regulated by SbtR (Fig. 5).

The transcriptional start sites of the SbtR-regulated genes *in vivo* were determined by 5′-RACE analyses. They were found downstream of the predicted SbtR-binding sites [Fig. 5(A)]. Note that among the 13 sequenced clones, the transcriptional start site of the *TTHA0787* gene, C (+1), was converted to T in nine of them, and to G in three. In the case of the *TTHA1821* gene, the transcriptional start site of one of the four clones was identified at the G (-1) site, and was converted to A. As for the *TTHA1822* gene, it was converted to A in one of the four clones. The potential promoter sequences were found within or in close proximity to the predicted SbtR-binding sites [Fig. 5(A)]. These results agreed well with those from the *in vitro* transcription assays, and supported the proposed function of SbtR as a transcriptional repressor of these genes. We investigated the operon structure of the SbtR-regulated genes by an RT-PCR analysis. We found that the *TTHA0787–TTHA0785*, *TTHA1822–TTHA1823*, and *TTHA1821–TTHA1818* genes form operons [Fig. 5(B)]. Thus, the 10 genes summarized in Table II may be negatively regulated by SbtR. The functions of the SbtR-regulated gene products, as predicted from their amino acid sequences, are summarized in Table II.

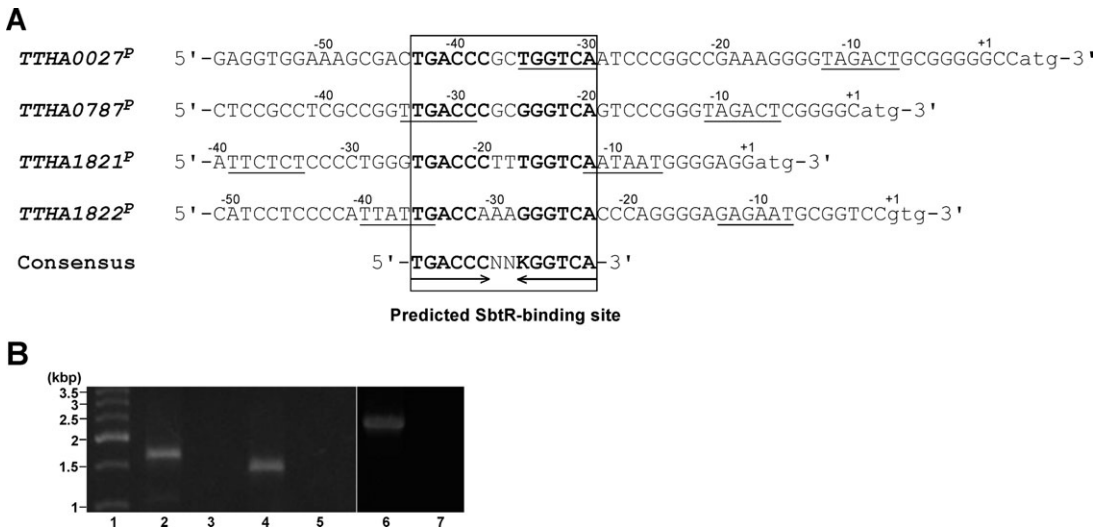

Figure 5

(**A**) Nucleotide sequence alignment of the promoters regulated by *T. thermophilus* SbtR. *TTHA0027*^{P}, *TTHA0787*^{P}, *TTHA1821*^{P}, and *TTHA1822*^{P} denote the promoter regions of the *TTHA0027*, *TTHA0787*, *TTHA1821*, and *TTHA1822* genes, respectively. The predicted SbtR-binding sites and the consensus sequence are indicated. The conserved bases in the SbtR binding sites are indicated by bold letters. Possible –10 and –35 hexamer sequences in the promoters are underlined. The transcription start site of each gene (+1), as determined by a 5′-RACE experiment, is indicated. Among the 13 sequenced clones, the transcriptional start site of the *TTHA0787* gene, C (+1), was converted to T in nine of them, and to G in three. In the case of the *TTHA1821* gene, the transcriptional start site of one of the four clones was identified at the G (−1) site, and was converted to A. As for the *TTHA1822* gene, the transcriptional start site was converted to A in one of the four clones. (**B**) RT-PCR analysis to confirm the operons composed of the *TTHA0787–TTHA0785* (lane 2), *TTHA1822–TTHA1823* (lane 4), and *TTHA1821–TTHA1818* (lane 6) genes. As a control, PCR was also performed with no RT, using the same primers (lanes 3, 5, and 7). The samples were fractionated on a 1% agarose gel, which was stained with ethidium bromide and photographed. Lane 1, 500-bp DNA ladder markers.

Three-dimensional structure of T. thermophilus SbtR

The crystal structure of SbtR, produced in *E. coli*, was determined by the SAD method, and was refined to 2.05-Å resolution, with crystallographic R_{work} and R_{free} factors of 20.1 and 25.0%, respectively (Table I). The asymmetric unit of the crystal comprised two homodimers (chains A:B and C:D) of SbtR. The overall structure of SbtR is shown in Figure 6(A). The final model exhibits the three-dimensional structure of a typical TetR family protein, and contains nine (chains A, B, and D) or 10 (chain C) α-helices [Figs. 1 and 6(A)].[4] Note that several disordered

Table II
Features of the *T. thermophilus* SbtR-Regulated Gene Products

Gene	Annotation for product	Domain	*E* value to the domain
TTHA0027	Potassium channel subunit beta	Predicted oxidoreductases (related to aryl-alcohol dehydrogenases) (COG0667)	2.18e-101
		Aldo-keto reductases (cd06660)	3.82e-101
TTHA0785	Hypothetical protein	Sulfite exporter TauE/SafE (pfam01925)	5.69e-13
TTHA0786	Glycerate dehydrogenase/glyoxylate reductase	Lactate dehydrogenase and related dehydrogenases LdhA (COG1052)	1.76e-90
		Glyoxylate reductase (PRK13243)	6.70e-85
TTHA0787	Hypothetical protein	–	–
TTHA1818	Recombinase A	RecA (cd00983)	6.04e-139
TTHA1819	2′-5′ RNA ligase	2′-5′ RNA ligase LigT (COG1514)	7.33e-31
TTHA1820	Competence/damage-inducible protein CinA	Competence damage-inducible protein A (PRK00549)	3.49e-105
TTHA1821	Glycine cleavage system protein T (folate-binding aminomethyltransferase)	Folate-binding protein YgfZ (TIGR03317)	1.76e-11
		Predicted aminomethyltransferase related to GcvT (COG0354)	1.34e-10
TTHA1822	Transporter	–	–
TTHA1823	Hydrolase	Predicted phosphatase/phosphohexomutase (COG0637)	7.22e-43
		Haloacid dehalogenase-like hydrolase family protein (PLN02770)	5.74e-40

A BLAST search was performed for each gene product, and the representative conserved domain and *E* value to the domain are shown.

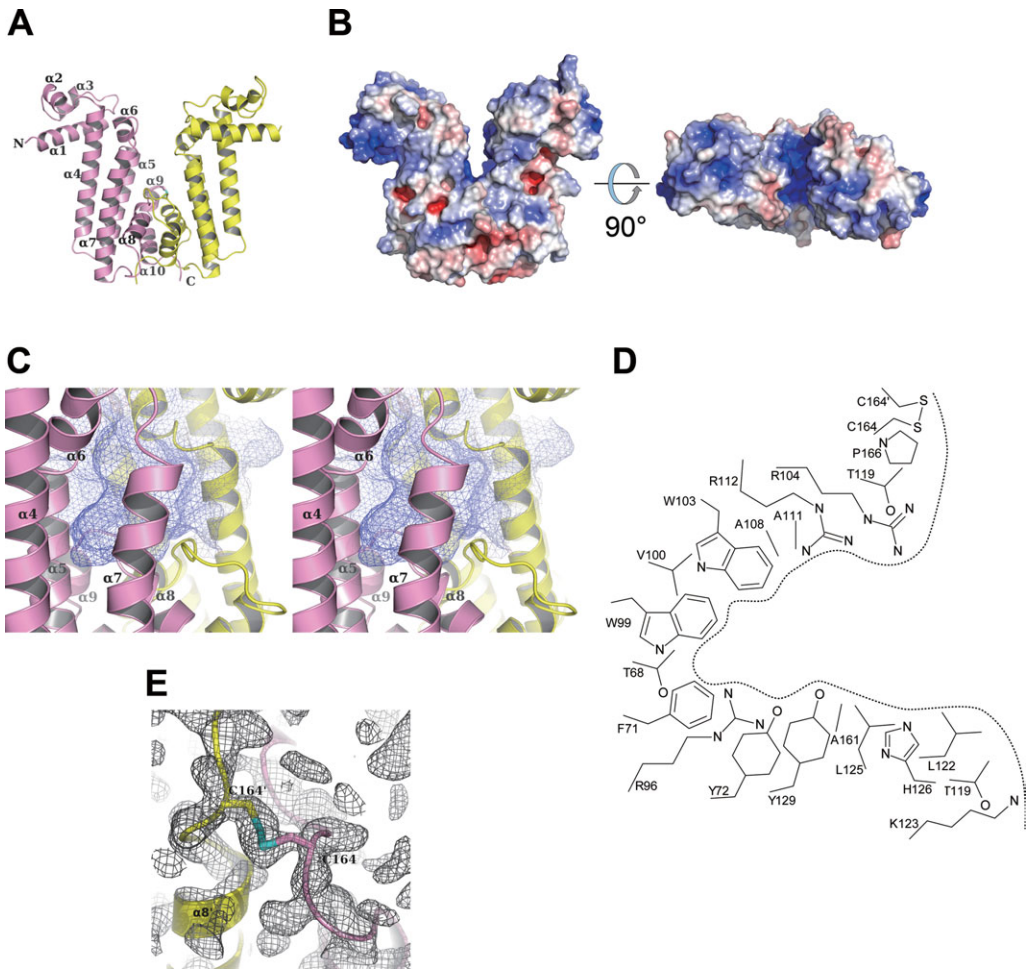

Figure 6

X-ray crystal structure of *T. thermophilus* SbtR. (**A**) Ribbon diagram of the SbtR dimer [chains C (pink) and D (yellow)]. (**B**) Molecular surface representation of the SbtR dimer. Red and blue surfaces represent negative and positive electrostatic potentials ($-5\ k_BT$, $+5\ k_BT$), respectively. The electrostatic potentials were calculated using the Adaptive Poisson–Boltzmann Solver (APBS),[32] with the PyMol APBS tools. (**C**) Stereoview of the center of the SbtR molecule. Chains C and D are shown in pink and yellow, respectively. The putative ligand-binding pocket is indicated by a mesh. (**D**) Schematic model structures of the residues comprising the putative ligand-binding pocket of SbtR. (**E**) The $|F_o - F_c|$ omit electron density map (gray mesh) around the disulfide bridge between Cys164 on chains C (pink) and Cys164′ on chain D (yellow), contoured at 1.5 σ. All of these figures, except for (D), were drawn using the PyMol program (http://www.pymol.org/).

regions are not included in the model; i.e., Ala1–Gly7, Leu168, and Glu169 for chain A; Ala1–Gly7 and Pro166–Glu169 for chain B; Ala1–Ala8 for chain C; and Ala1–Gly9 for chain D. The α9 helices are not observed at the corresponding regions of chains A, B, and D. The root mean square deviation (r.m.s.d.) values between chains C and B, chains C and A, and chains C and D are 1.0, 1.8, and 3.1 Å, respectively. The structure of SbtR was compared with those in the PDB database, using the PDBeFold server (http://www.ebi.ac.uk/msd-srv/ssm/). The closest structures to chain C were the TetR/AcrR family transcriptional regulator from *Bacillus subtilis* str. 168 [PDB code: 2F07, Z = 5.9, r.m.s.d. = 2.8 Å, number of matched residues = 179, sequence identity (IDE) = 19%], and the TetR family transcriptional regulator from *Mycobacterium vanbaalenii* PYR-1 (PDB code: 2QWT, Z = 5.3, r.m.s.d. = 2.8 Å, number of matched residues = 152, IDE = 26%). The closest structures to chain D were *Mycobacterium tuberculosis* EthR in complex with hexadecyl octanoate (PDB code: 1U9O, Z = 4.8, r.m.s.d. = 2.8 Å, number of matched residues = 162, IDE = 15%), and the TetR family transcriptional regulator from *Archaeoglobus fulgidus* DSM 4304 (PDB code 3EGQ, Z = 5.0, r.m.s.d. = 2.5 Å, number of matched residues = 137, IDE = 22%). The TetR family transcriptional regulator from *M. vanbaalenii* PYR-1 (PDB code 2QWT) has a cysteine residue close to the corresponding position of Cys164 in

SbtR (Fig. 1), but the three-dimensional structure around the cysteine residue could not be determined from the coordinates.

The N-terminal domain (α1–α3) of SbtR, containing the typical HTH motif (α2–α3) with a positively charged surface [Fig. 6(B)], may be the DNA-binding domain, as in the cases of other TetR family proteins.[4] All of the characterized TetR family regulators bind small molecules as ligands in similarly positioned pockets, around the center of the molecule.[4] In the SbtR structure, a comparable pocket exists at the center of each monomer molecule [Fig. 6(C)]. The pocket comprises aromatic residues (Trp and Phe), hydrophobic residues (Tyr and Leu), and polar residues (His and Arg) [Fig. 6(D)]. These are common features of the ligand-binding pockets of several TetR family regulators.[4] Excess electron density was not observed in the pocket of SbtR, suggesting that this structure is the ligand-free form. An intermolecular disulfide bridge between the Cys164 residues on the loops between α8 and α9 (or α10) was detected at the entrance of the pocket [Fig. 6(D,E)]. The conformation of the N-terminal domain relative to the C-terminal domain slightly differed among the chains (Supporting Information Fig. S3), supporting the previous finding that the ligand-free form of the TetR family regulator is flexible.[8,9] The distance between the two Cα atoms of the amino acid residues located in the center of the α3 helices of SbtR (Tyr50), which may interact with the major groove of the DNA, is ~51–53 Å. This distance is greater than those of the DNA-binding forms of other typical TetR family regulators; i.e., *E. coli* TetR (35 Å),[5] *Staphylococcus aureus* QacR (37 Å),[33] *Streptomyces antibioticus* SimR (37 Å),[34] and *Corynebacterium glutamicum* CgmR (44 Å).[35] If the ligand-free form of SbtR is flexible, then the structure that is compatible with DNA binding might differ from that determined in this study.[9,34]

Effect of the Cys164 mutation on the stability and activity of SbtR

To investigate the importance of the disulfide bridge with respect to the stability and activity of SbtR, the C164S and C164A mutant proteins were prepared (Supporting Information Fig. S4). We assessed the properties of these mutants because the disulfide bridge was not completely cleaved, even in the presence of excess amounts of a reductant (Fig. 2). The molecular masses of both proteins, as estimated by gel-filtration chromatography, were ~40 kDa (Supporting Information Fig. S1), suggesting that the mutant proteins exist as homodimers in solution, as in the case of the wild type, and that the disulfide bridge is not required for SbtR dimerization. Next, we performed DSC measurements to compare the thermal stabilities of the mutants with that of the wild type (Fig. 7). The peak temperature of the wild type was 98.5°C, while those of the C164S and C164A mutants were 90.8 and 90.1°C, respectively, suggesting that the intermolecular disulfide bridge contributes to the increased thermal stability of SbtR.

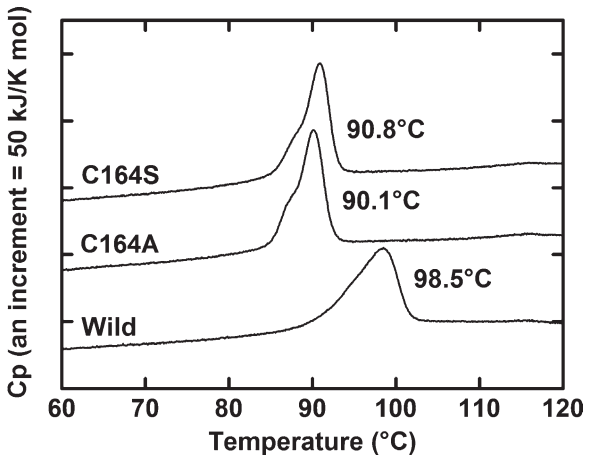

Figure 7

Typical DSC curves of the wild-type and the C164S and C164A mutant SbtR proteins at pH 7.0. The DSC heating rate was 1°C min^{-1} for each analysis. Representative results are shown. The peak temperature of each protein is indicated.

The transcriptional repression activities of the mutant proteins were almost the same as that of the wild-type protein *in vitro* (Supporting Information Fig. S5). The ITC measurements demonstrated that the mutant SbtR proteins bound the dsDNA containing the SbtR-binding site with several-fold lower K_d values at 15°C (data not shown), as compared to that of the wild-type protein. On the other hand, the BIAcore analyses revealed that, as compared to the wild-type protein, the mutant SbtR proteins bound the DNA with several-fold higher K_d values, which were mainly attributed to the increased k_{off} values of the mutant proteins (data not shown).

DISCUSSION

The X-ray crystal structure analysis revealed that the three-dimensional structure of one of the four TetR family transcriptional regulators of *T. thermophilus* HB8, which we named *T. thermophilus* SbtR, is similar to those of numerous characterized TetR family regulators.[4] Many of the characterized TetR family regulators bind small molecules as ligands in similarly positioned pockets near the center of the molecules, and the ligand-binding induces derepression of the regulators.[4] In the SbtR structure, a comparable pocket exists at the center of each monomer molecule, and it may be a ligand-binding site, because its position and the residues comprising the pocket resemble those of the characterized TetR family regulators.[4] SbtR, like other characterized TetR family regulators, may bind a ligand to derepress its target

genes. Interestingly, an intermolecular disulfide bridge is formed via the Cys164 residues, at the interface of the dimer molecules. We found that the disulfide bridge contributed to the thermal stability of SbtR. The C164S and C164A mutant SbtR proteins formed homodimers, as in the case of the wild-type protein, and the mutant proteins displayed almost the same transcriptional repression activity as that of the wild type *in vitro*. These results suggested that the repressive mechanism is essentially unaltered, even if the intermolecular disulfide bridge is absent. We detected different DNA-binding strengths of the mutant SbtR proteins relative to that of wild type, depending on the method of measurement; i.e., the binding affinities of the mutants were higher than that of the wild-type in the ITC measurement, but lower in the BIAcore analysis. We are not sure whether the intermolecular disulfide bridge is actually formed in *T. thermophilus* cells, and if its formation or reduction contributes to the function of this protein. However, since the disulfide bridge resides at the entrance of the putative-ligand pocket, and the mutants lacking the disulfide bridges exhibited lower thermal stability *in vitro*, the formation and reduction of the disulfide bond may play roles in both the activity and stability of this transcriptional regulator *in vivo*. Because the repressive activity of the mutant SbtR proteins lacking the cysteine residues was retained, ligand-binding may be essential for the derepression of SbtR. The formation or reduction of the disulfide bond in SbtR may facilitate ligand binding. If so, then the expression of SbtR-regulated genes might differ depending on the redox conditions, even in the presence of the SbtR ligand.

In an *in vitro* study, we found that *T. thermophilus* SbtR transcriptionally repressed 10 genes. The gene products included probable transporters, probable enzymes for sugar or amino acid metabolism, and nucleic acid-related enzymes. In the *T. thermophilus* genome, *carD* [also called the *cdnL* (*TTHA0168*) gene], a homolog of *Mycobacterium carD*,[36] is located downstream of the *sbtR* gene, and they could form an operon (NCBI accession number NC_006461), suggesting that these genes are functionally relevant. The CarD (CdnL) protein is an RNA polymerase modulator that is widely distributed in bacteria.[37] In *Mycobacterium* species, CarD controls rRNA transcription, and is involved in the oxidative stress response, the DNA damage response, and starvation.[36] *T. thermophilus* CarD[36] might perform similar functions in coordination with SbtR, because one of the target gene products of SbtR was RecA, which is involved in DNA repair. If *T. thermophilus* CarD and SbtR are involved in the oxidative stress response, as in the case of *Mycobacterium* CarD, then the reduction and formation of the intermolecular disulfide bond of SbtR might occur *in vivo*, to respond to the stress. In support of this proposal, we found that the *TTHA0164* gene, encoding a thiol:disulfide interchange protein that might be involved in the oxidative stress response, is located close to the *sbtR* gene, although it was not regulated by SbtR. The *carD-sbtR* genes are conserved only in the *Thermus*, *Meiothermus*, and *Oceanithermus* species; thus, the functional coordination between CarD and SbtR could only occur in these species. The TetR family regulator CprB, from *Streptomyces coelicolor* A3(2), also contains an intermolecular disulfide bridge at a similar position.[10] This protein controls antibiotic production and/or morphogenesis. Thus, the cellular or physiological roles of the TetR-family protein-regulated gene products may differ, even though the cognate transcriptional regulators share similar disulfide bridges.

Further research on SbtR and its regulated gene products will be necessary to elucidate the cellular roles of this transcriptional regulator, as well as its mechanisms of transcriptional repression and derepression.

ACKNOWLEDGMENTS

The authors thank Aimi Osaki for the construction of the expression plasmids encoding the mutant SbtR proteins. They thank Kayoko Matsumoto for protein purification, Toshi Arima for crystallization, and Michiyo Takehira for ITC and DSC measurements. They also thank Drs. Hitoshi Iino and Kenji Fukui for data collection at SPring-8.

REFERENCES

1. Minezaki Y, Homma K, Nishikawa K. Genome-wide survey of transcription factors in prokaryotes reveals many bacteria-specific families not found in archaea. DNA Res 2005;12:269–280.
2. Ramos JL, Martinez-Bueno M, Molina-Henares AJ, Teran W, Watanabe K, Zhang X, Gallegos MT, Brennan R, Tobes R. The TetR family of transcriptional repressors. Microbiol Mol Biol Rev 2005;69:326–356.
3. Rodionov DA. Comparative genomic reconstruction of transcriptional regulatory networks in bacteria. Chem Rev 2007;107:3467–3497.
4. Yu Z, Reichheld SE, Savchenko A, Parkinson J, Davidson AR. A comprehensive analysis of structural and sequence conservation in the TetR family transcriptional regulators. J Mol Biol 2010;400:847–864.
5. Orth P, Schnappinger D, Hillen W, Saenger W, Hinrichs W. Structural basis of gene regulation by the tetracycline inducible Tet repressor-operator system. Nat Struct Biol 2000;7:215–219.
6. Schumacher MA, Miller MC, Grkovic S, Brown MH, Skurray RA, Brennan RG. Structural mechanisms of QacR induction and multidrug recognition. Science 2001;294:2158–2163.
7. Willems AR, Tahlan K, Taguchi T, Zhang K, Lee ZZ, Ichinose K, Junop MS, Nodwell JR. Crystal structures of the *Streptomyces coelicolor* TetR-like protein ActR alone and in complex with actinorhodin or the actinorhodin biosynthetic precursor (S)-DNPA. J Mol Biol 2008;376:1377–1387.
8. Le TB, Stevenson CE, Fiedler HP, Maxwell A, Lawson DM, Buttner MJ. Structures of the TetR-like simocyclinone efflux pump repressor, SimR, and the mechanism of ligand-mediated derepression. J Mol Biol 2011;408:40–56.
9. Reichheld SE, Yu Z, Davidson AR. The induction of folding cooperativity by ligand binding drives the allosteric response of tetracycline repressor. Proc Natl Acad Sci USA 2009;106:22263–22268.

10. Natsume R, Ohnishi Y, Senda T, Horinouchi S. Crystal structure of a gamma-butyrolactone autoregulator receptor protein in *Streptomyces coelicolor* A3(2). J Mol Biol 2004;336:409–419.
11. Oshima T, Imahori K. Description of *Thermus thermophilus* (Yoshida and Oshima) com. nov., a non-sporulating thermophilic bacterium from a Japanese thermal spa. Int J Syst Bacteriol 1974;24:102–112.
12. Ohtani N, Tomita M, Itaya M. The third plasmid pVV8 from *Thermus thermophilus* HB8: isolation, characterization, and sequence determination. Extremophiles 2012;16:237–244.
13. Agari Y, Agari K, Sakamoto K, Kuramitsu S, Shinkai A. TetR family transcriptional repressor *Thermus thermophilus* FadR controls fatty acid degradation. Microbiology 2011;157:1589–1601.
14. Sakamoto K, Agari Y, Kuramitsu S, Shinkai A. Phenylacetyl coenzyme A is an effector molecule of the TetR family transcriptional repressor PaaR from *Thermus thermophilus* HB8. J Bacteriol 2011;193:4388–4395.
15. Agari Y, Sakamoto K, Kuramitsu S, Shinkai A. Transcriptional repression mediated by a TetR family protein, PfmR, from *Thermus thermophilus* HB8. J Bacteriol 2012;194:4630–4641.
16. Lemaster DM, Richards FM. ^{1}H-^{15}N heteronuclear NMR studies of *Escherichia coli* thioredoxin in samples isotopically labeled by residue type. Biochemistry 1985;24:7263–7268.
17. Kuramitsu S, Hiromi K, Hayashi H, Morino Y, Kagamiyama H. Pre-steady-state kinetics of *Escherichia coli* aspartate aminotransferase catalyzed reactions and thermodynamic aspects of its substrate specificity. Biochemistry 1990;29:5469–5476.
18. Ueno G, Kanda H, Hirose R, Ida K, Kumasaka T, Yamamoto M. RIKEN structural genomics beamlines at the SPring-8; high throughput protein crystallography with automated beamline operation. J Struct Funct Genomics 2006;7:15–22.
19. Otwinowski Z, Minor W. Processing of X-ray diffraction data collected in oscillation mode. Methods Enzymol 1997;276:307–326.
20. Terwilliger TC, Berendzen J. Automated MAD and MIR structure solution. Acta Crystallogr D Biol Crystallogr 1999;55:849–861.
21. Perrakis A, Harkiolaki M, Wilson KS, Lamzin VS. ARP/wARP and molecular replacement. Acta Crystallogr D Biol Crystallogr 2001;57:1445–1450.
22. Collaborative Computational Project Number 4. The CCP4 suite: programs for protein crystallography. Acta Crystallogr D Biol Crystallogr 1994;50:760–763.
23. Emsley P, Cowtan K. *Coot*: model-building tools for molecular graphics. Acta Crystallogr D Biol Crystallogr 2004;60:2126–2132.
24. Brünger AT, Adams PD, Clore GM, Delano WL, Gros P, Grosse-Kunstleve RW, Jiang JS, Kuszewski J, Nilges M, Pannu NS, Read RJ, Rice LM, Simonson T, Warren GL. Crystallography and NMR system: a new software suite for macromolecular structure determination. Acta Crystallogr D Biol Crystallogr 1998;54:905–921.
25. Shimada T, Fujita N, Maeda M, Ishihama A. Systematic search for the Cra-binding promoters using genomic SELEX system. Genes Cells 2005;10:907–918.
26. Shinkai A, Kira S, Nakagawa N, Kashihara A, Kuramitsu S, Yokoyama S. Transcription activation mediated by a cyclic AMP receptor protein from *Thermus thermophilus* HB8. J Bacteriol 2007;189:3891–3901.
27. Vassylyeva MN, Lee J, Sekine SI, Laptenko O, Kuramitsu S, Shibata T, Inoue Y, Borukhov S, Vassylyev DG, Yokoyama S. Purification, crystallization and initial crystallographic analysis of RNA polymerase holoenzyme from *Thermus thermophilus*. Acta Crystallogr D Biol Crystallogr 2002;58:1497–1500.
28. Goujon M, Mcwilliam H, Li W, Valentin F, Squizzato S, Paern J, Lopez R. A new bioinformatics analysis tools framework at EMBL-EBI. Nucleic Acids Res 2010;38:W695–W699.
29. Sievers F, Wilm A, Dineen D, Gibson TJ, Karplus K, Li W, Lopez R, Mcwilliam H, Remmert M, Soding J, Thompson JD, Higgins DG. Fast, scalable generation of high-quality protein multiple sequence alignments using Clustal Omega. Mol Syst Biol 2011;7:539.
30. Kabsch W, Sander C. Dictionary of protein secondary structure: pattern recognition of hydrogen-bonded and geometrical features. Biopolymers 1983;22:2577–2637.
31. Gouet P, Robert X, Courcelle E. ESPript/ENDscript: extracting and rendering sequence and 3D information from atomic structures of proteins. Nucleic Acids Res 2003;31:3320–3323.
32. Baker NA, Sept D, Joseph S, Holst MJ, Mccammon JA. Electrostatics of nanosystems: application to microtubules and the ribosome. Proc Natl Acad Sci USA 2001;98:10037–10041.
33. Schumacher MA, Miller MC, Grkovic S, Brown MH, Skurray RA, Brennan RG. Structural basis for cooperative DNA binding by two dimers of the multidrug-binding protein QacR. EMBO J 2002;21:1210–1218.
34. Le TB, Schumacher MA, Lawson DM, Brennan RG, Buttner MJ. The crystal structure of the TetR family transcriptional repressor SimR bound to DNA and the role of a flexible N-terminal extension in minor groove binding. Nucleic Acids Res 2011;39:9433–9447.
35. Itou H, Watanabe N, Yao M, Shirakihara Y, Tanaka I. Crystal structures of the multidrug binding repressor *Corynebacterium glutamicum* CgmR in complex with inducers and with an operator. J Mol Biol 2010;403:174–184.
36. Stallings CL, Stephanou NC, Chu L, Hochschild A, Nickels BE, Glickman MS. CarD is an essential regulator of rRNA transcription required for *Mycobacterium tuberculosis* persistence. Cell 2009;138:146–159.
37. Stallings CL, Glickman MS. CarD: a new RNA polymerase modulator in mycobacteria. Transcription 2011;2:15–18.